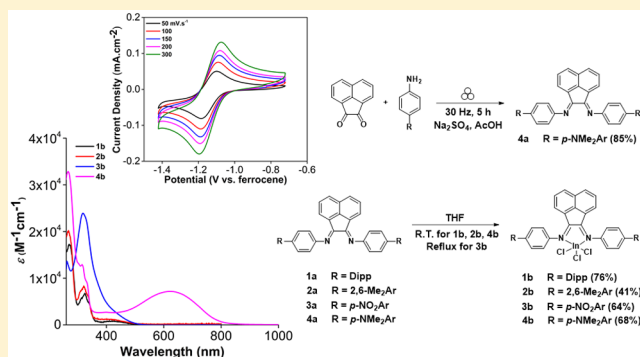


## Synthesis and the Optical and Electrochemical Properties of Indium(III) Bis(arylimino)acenaphthene Complexes

Jingyi Wang,<sup>†</sup> Rakesh Ganguly,<sup>†</sup> Li Yongxin,<sup>†</sup> Jesus Díaz,<sup>\*,‡</sup> Han Sen Soo,<sup>\*,†,§,||</sup> and Felipe García<sup>\*,†</sup><sup>†</sup>Division of Chemistry and Biological Chemistry, School of Physical and Mathematical Sciences, Nanyang Technological University, 21 Nanyang Link, 637371, Singapore<sup>‡</sup>Departamento de Química Orgánica e Inorgánica, Facultad de Veterinaria, Universidad de Extremadura, Cáceres 10071, Spain<sup>§</sup>Singapore-Berkeley Research Initiative for Sustainable Energy (SinBeRISE), 1 Create Way, 138602 Singapore<sup>||</sup>Solar Fuels Laboratory, Nanyang Technological University, 50 Nanyang Avenue, 639798 Singapore

## S Supporting Information

**ABSTRACT:** Aryl bis(imino)acenaphthenes (Ar-BIANs) are well-established rigid and sterically bulky diimine ligands, which are redox-noninnocent and versatile  $\pi$ -acceptors due to their low-lying  $\pi^*$  orbitals and are frequently used to bind transition metals. However, the coordination chemistry of Ar-BIAN ligands to main group elements is not as well-developed as that of their transition metal counterparts. In particular, there are no comprehensive studies describing the spectroscopic and electrochemical properties of main group Ar-BIAN complexes. Herein, we report the synthesis and full characterization of a series of new indium(III) Ar-BIAN complexes, bearing 2,6-dialkyl (**1b** and **2b**), 4-nitro (**3b**), and 4-dimethylamino (**4b**) groups at the aryl-diimine part of the ligand. Their optical and electrochemical properties have been revealed by UV-vis spectroscopy and cyclic voltammetry, respectively. Additionally, DFT calculations were performed to gain insights into the nature of the properties displayed.



## INTRODUCTION

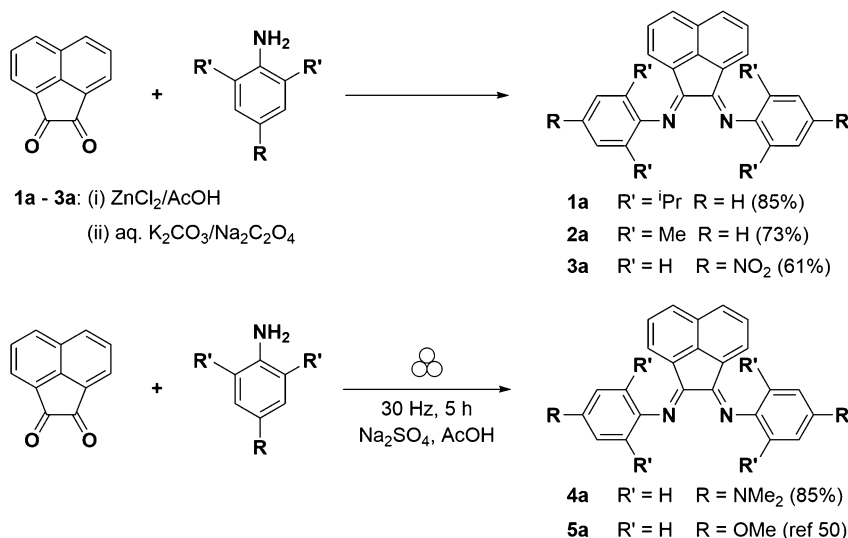
Redox processes and redox-active ligands play important roles in modern chemical transformations constituting exciting areas of research in coordination and organometallic chemistry,<sup>1</sup> and catalysis.<sup>2</sup> The term “innocent ligand” was first coined by Jørgensen as a ligand that allows the oxidation states of the central atoms to be readily determined.<sup>3</sup> In contrast, “non-innocent ligands” refer to ligands in metal complexes where the oxidation states are ambiguous and need to be experimentally determined.<sup>1</sup> Noninnocent ligands have energetically accessible electronic levels rendering these species redox active at mild potentials.<sup>4</sup> Aryl bis(imino)acenaphthenes (Ar-BIAN) belong to one class of noninnocent ligands. Ar-BIAN ligands were first reported in the 1960s and have been widely investigated as robust ligands for catalytically active transition metal centers since the early 1990s.<sup>5</sup> Although many coordination complexes between transition metal and Ar-BIAN ligands have been described,<sup>6–10</sup> their main group and lanthanide counterparts remain poorly explored, with a limited selection of main group Ar-BIAN complexes being synthesized and crystallographically characterized.<sup>11,12</sup>

Ar-BIAN ligands are highly tunable species that are readily synthesized from cheap and commercially available anilines and acenaphthenequinone.<sup>13,14</sup> Functionalized Ar-BIAN compounds are acknowledged as oxidatively and thermally stable

ligands for transition metal centers. The extensive  $\pi$ -system of the acenaphthene ring combined with the sterically modular aniline provide a broad range of  $\pi$ -acceptor frameworks, offering precise control over the steric, optical, and electronic properties.<sup>14,15</sup> Consequently, Ar-BIAN ligands have been employed in the preparation of numerous transition metal molecular compounds, which could be of use in photo-sensitization applications due to the characterized MLCT (metal-to-ligand charge transfer) transition from the d-orbitals of the transition metal to the  $\pi^*$  orbitals of the Ar-BIAN ligand.<sup>9,10,16</sup> The low-lying  $\pi^*$  orbitals of Ar-BIAN ligands have been successfully exploited as “capacitors” for multielectron reductions in redox noninnocent ligands.<sup>17–19</sup> Consequently, there have been reports of transition metal Ar-BIAN complexes being used as catalysts for organic reactions such as cycloaddition of azides and alkynes,<sup>7,8</sup> as well as olefin polymerization, work that had been pioneered by Brookhart and co-workers using Ni(II) and Pd(II) Ar-BIAN complexes.<sup>20–27</sup> More recently, Cu(II) Ar-BIAN complexes have been investigated as catalysts for the reverse atom transfer radical polymerization (ATRP) of styrene.<sup>28</sup> Moreover,

Received: March 2, 2017



Scheme 1. General Synthetic Scheme of Ar-BIAN Ligands 1a–5a<sup>a</sup>

<sup>a</sup>The symbol for mechanical milling above the arrow of the equation in the lower half has been proposed by Hanusa et al.<sup>58</sup>

applications of Cu(I) Ar-BIAN complexes as light harvesters that can absorb to the NIR region have also been reported.<sup>6,9,16</sup>

In terms of main group chemistry, however, groups 1 and 2 constitute the majority of the Ar-BIAN main group metal complexes.<sup>17–19,29–35</sup> In these examples, each Ar-BIAN ligand undergoes facile reduction due to its electron accepting nature to form the corresponding metal complex.<sup>11</sup> With respect to group 14 metals, a small number of complexes have been previously reported. For instance, *N*-heterocyclic gemylenes that contain anionic Ar-BIAN ligands include [(dipp-BIAN)-Ge:], [(dtb-BIAN)Ge:] (dipp = 2,6-diisopropylphenyl, dtb = 2,5-*t*-Bu<sub>2</sub>Ph), and [(bph-BIAN)Ge:] (bph = (2-PhC<sub>6</sub>H<sub>4</sub>)).<sup>36</sup> Moreover, complexes such as (dipp-BIAN)GeCl have been prepared by reacting the neutral Ar-BIAN ligands with GeCl<sub>2</sub>, where GeCl<sub>2</sub> acts as a reducing agent for the Ar-BIAN ligands to form their radical anionic counterparts.<sup>37,38</sup> On going down this group, tin complexes supported by neutral Ar-BIAN ligands have also been described, including [(mes-BIAN)SnCl<sub>4</sub>] (mes = 2,4,6-trimethylphenyl) and [(dtb-BIAN)SnCl<sub>2</sub>].<sup>12,38,39</sup> A series of group 15 and 16 Ar-BIAN metal complexes have been previously characterized as well. For example, [(dipp-BIAN)-SbCl<sub>3</sub>] and [(mes-BIAN)BiCl<sub>3</sub>]<sup>12</sup> supported by neutral Ar-BIAN ligands, and [(dipp-BIAN)E] [SnCl<sub>5</sub>·THF] obtained by reduction of ECl<sub>3</sub> (E = P and As) with SnCl<sub>2</sub>, followed by treatment with dipp-BIAN to give their dianionic form.<sup>40</sup> As for the chalcogens, the reaction of TeI<sub>4</sub> with neutral dipp-BIAN results in a two-electron reduction of the metal center to form [(dipp-BIAN)TeI<sub>2</sub>], in which the ligand is neutral and the chalcogen has been reduced to the +2 oxidation state.<sup>41</sup> More recently, the (dipp-BIAN)SeCl<sub>2</sub> and (dipp-BIAN)SeBr<sub>2</sub> counterparts have also been described.<sup>42</sup> Clearly, the redox noninnocence of Ar-BIAN ligands have contributed to some rich chemistry and oxidation state ambiguity even among main group coordination compounds.

In the case of group 13 complexes, other than a limited number of boron compounds,<sup>39,43</sup> only a few aluminum and gallium Ar-BIAN complexes have been isolated and structurally characterized.<sup>43–49</sup> In particular, until very recently,<sup>50</sup> there was only one crystallographically characterized example of a monometallic Ar-BIAN indium(III) complex<sup>12</sup> and two reports

presenting the related tetrakis(imino)py-racene (TIP) ligand.<sup>51</sup> Hence, the synthesis of new, heavy group 13 Ar-BIAN complexes and the evaluation of their absorption and electrochemical properties still remain under-explored areas.

Our group is interested in applying mechanochemical approaches to synthetic main group compounds<sup>52</sup> and has recently reported the preparation of new indium(III) bis-(arylimino)-acenaphthene complexes by using an essentially solvent-free mechanochemical approach.<sup>50</sup> The indium(III) complexes were characterized by density functional theory (DFT) calculations, electrochemistry, and UV–vis–NIR spectroscopy. The electrochemical data suggested that the Ar-BIAN indium(III) complexes could be converted to their indium(I) congeners by mild reducing agents, offering us the opportunity to explore the intriguing redox noninnocence of the Ar-BIAN systems. Upon reduction of the indium(III) center, these complexes show potential for applications as photosensitizers, dovetailing with our interest in the use of earth-abundant elements in artificial photosynthesis.<sup>16,53–55</sup>

Herein, we present a family of new indium(III) Ar-BIAN complexes with the synthesis of a broad range of Ar-BIAN ligands comprising electron-donating and -deficient substituents on the arylimino fragment. All of the complexes reported here have been structurally characterized and probed with electrochemical and UV–vis spectroscopic measurements, as well as DFT and TD-DFT calculations.

## RESULTS AND DISCUSSION

**Synthesis of Complexes.** The alkyl- and nitro-substituted Ar-BIAN ligands (1a–3a) were synthesized by condensation of acenaphthoquinone with the corresponding aniline under acidic conditions.<sup>56,57</sup> The Lewis acidic ZnCl<sub>2</sub> was used as the templating agent, after which demetalation with K<sub>2</sub>CO<sub>3</sub> or Na<sub>2</sub>C<sub>2</sub>O<sub>4</sub> was carried out (Scheme 1, top half). However, this method proved unsuccessful for the synthesis of *para*-amino-substituted 4a, and ligand hydrolysis was observed after the demetalation step in an aqueous Na<sub>2</sub>C<sub>2</sub>O<sub>4</sub> solution. Alternatively, we have previously demonstrated that substituted Ar-BIAN ligands can be successfully synthesized via mechanochemical methodologies, which bypass the ZnCl<sub>2</sub> templating

Scheme 2. Synthetic Route to 1b–5b

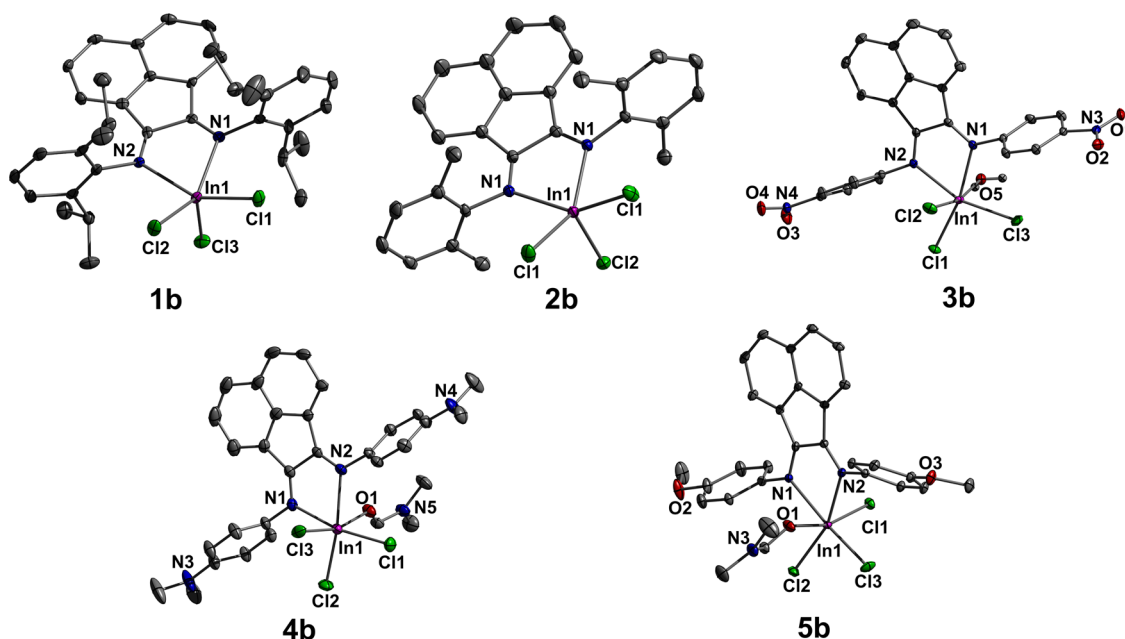
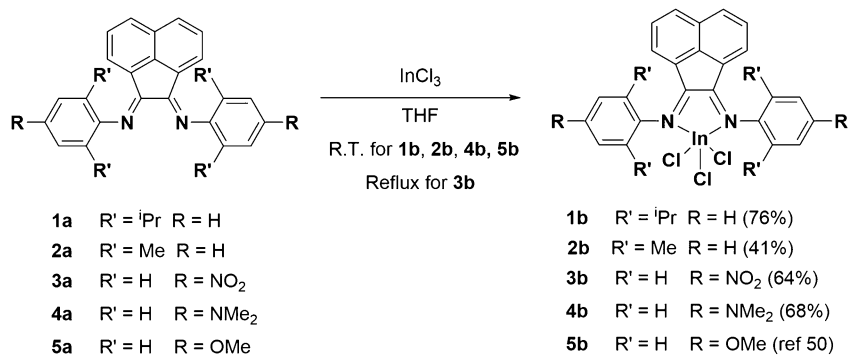


**Figure 1.** Selected bond lengths (Å) and angles (deg) of complexes (**1b**) In1–N1 2.342(5), In1–N2 2.339(5), In1–Cl1 2.3835(16), In1–Cl2 2.3800(17), In1–Cl3 2.3643(17); (**2b**) In1–N1 2.3196(15), In1–Cl1 2.3897(5), In1–Cl2 2.3769(7); (**3b**) In1–N1 2.3230(14), In1–N2 2.3114(14), In1–Cl1 2.4013(4), In1–Cl2 2.4722(5), In1–Cl3 2.4032(5), In1–O5 2.2733(13); (**4b**) In1–N1 2.317(3), In1–N2 2.331(3), In1–Cl1 2.4029(10), In1–Cl2 2.4241(9), In1–Cl3 2.4408(10), In1–O1 2.259(3); (**5b**) In1–N1 2.3182(14), In1–N2 2.3444(13), In1–Cl1 2.4417(4), In1–Cl2 2.4301(4), In1–Cl3 2.4058(5), In1–O1 2.2306(13). Thermal ellipsoids are drawn at the 50% probability level. Hydrogen atoms have been omitted for clarity.

and subsequent demetalation step.<sup>50</sup> Accordingly, **4a** was prepared via a ball-milling mechanochemical approach in the presence of a catalytic amount of acetic acid and Na<sub>2</sub>SO<sub>4</sub> (Scheme 1, bottom half). The synthesis of **5a**, which we previously reported, has been included in Scheme 1 for the completeness of our study.<sup>50</sup> In a typical procedure, all reactants and additives were loaded into a stainless-steel grinder jar containing a 10 mm stainless steel ball (4 g weight). The reaction mixture was milled for 5 h in a Retsch MM400 mixer mill operating at 30 Hz.<sup>58,59</sup> On the basis of the <sup>1</sup>H NMR spectra, **4a** was formed with only trace amounts of unreacted precursors. Subsequent reaction of the Ar-BIAN ligand (**1a**–**5a**) with InCl<sub>3</sub> in tetrahydrofuran (THF) afforded the respective indium(III) Ar-BIAN complexes (**1b**–**5b**). The syntheses of **1b**, **2b**, **4b**, and **5b**<sup>60</sup> were conducted at room temperature, whereas **3b** was prepared under reflux conditions in THF (Scheme 2).

**Spectroscopic and Crystallographic Studies.** The <sup>1</sup>H and <sup>13</sup>C{<sup>1</sup>H} NMR spectra obtained for **1b**–**5b** concurred with

the formation of coordinated, neutral Ar-BIAN ligands on indium(III). In general, the <sup>1</sup>H NMR spectra of the coordinated Ar-BIAN ligands in complexes **1b**–**5b** each exhibit a downfield shift compared to the corresponding spectra of ligands **1a**–**5a**. Compounds **1b** and **2b** were purified by recrystallization from 1,2-dimethoxyethane (DME) and tetrahydrofuran (THF), respectively. In the case of **3b**, single crystals suitable for single-crystal X-ray diffraction analysis were obtained by recrystallization from acetonitrile (ACN); however, batch purification was carried out by slow diffusion of diethyl ether (Et<sub>2</sub>O) into DMF. Therefore, the characteristic DMF signals were present in the <sup>1</sup>H NMR spectrum of **3b** recorded in deuterated acetone (Figure S5). In the case of **4b** and **5b**, vapor diffusion of Et<sub>2</sub>O into DMF has been used for recrystallization and, hence, one DMF molecule is coordinated to each indium(III) metal center. Thus, the <sup>1</sup>H NMR spectra for both complexes reveal signals corresponding to DMF (Figures S6 and S8).

All indium(III) Ar-BIAN complexes were successfully recrystallized to provide samples suitable for single-crystal X-ray structural analyses (Figure 1). We have already previously reported two structures,  $[(p\text{-MeOAr-BIAN})_2\text{InCl}_2]^+[\text{InCl}_4]^-$  (**6**) and  $(p\text{-BrAr-BIAN})\text{InCl}_3$  (**7**), which we compare with and refer to in this report for the completeness of our studies.<sup>50</sup> Compound  $[(p\text{-MeOAr-BIAN})_2\text{InCl}_2]^+[\text{InCl}_4]^-$  (**6**) was originally recrystallized from ACN; however, when **6** is recrystallized from a more strongly coordinating solvent like DMF, mono Ar-BIAN complex **5b** is formed. We attribute the formation of **5b** to the stronger coordinating ability of DMF compared to that of ACN. Coordinating solvents ( $\text{H}_2\text{O}$  for **3b**, DMF for **4b** and **5b**) are bound to each indium center resulting in distorted octahedral geometries for the complexes. The equatorial bond angles range from  $72.64(5)$  to  $101.06(2)^\circ$  in **3b**, from  $72.85(10)$  to  $97.94(8)^\circ$  in **4b**, and from  $72.68(5)$  to  $96.77(4)^\circ$  in **5b**, deviating significantly from the ideal value of  $90^\circ$ . Similarly, the axial bond angles ( $166.45(4)$ ,  $164.01(7)$ , and  $162.18(4)^\circ$  in **3b–5b**, respectively) also deviate from the expected  $180^\circ$ . This deviation of axial and equatorial bond angles in a distorted octahedral geometry was also reported in a similar *mes*-BIAN- $\text{InCl}_3$  complex.<sup>12</sup>

In contrast, **1b** and **2b** adopt distorted square pyramidal geometries presumably due to the increased steric hindrance around the metal nucleus introduced by substitution of isopropyl (in **1b**) and methyl (in **2b**) groups at the *ortho* positions of the aniline moiety. The axial bond angles range from  $95.89(13)$  to  $110.12(6)^\circ$  in **1b** and from  $100.86(4)$  to  $107.42(19)^\circ$  in **2b**, similar to those in the related tetrakis-(imino)pyracene (TIP) complexes that also adopt distorted square pyramidal geometries around the indium center ( $94.2\text{--}117.4^\circ$ ).<sup>51</sup> Complex **2b** exhibits a plane of symmetry bisecting the acenaphthene fragment and the indium metal center, making the two diimine N and Cl atoms at the equatorial positions equivalent. The C–C and C–N bond distances within the diimine moiety in **1b–5b** (ranging from  $1.517(3)$  to  $1.535(8)$  Å and from  $1.274(2)$  to  $1.288(4)$  Å, respectively) are consistent with typical C–C and C=N bond lengths.<sup>12</sup>

Therefore, complexes **1b–5b** can be considered to consist of neutral Ar-BIAN ligands coordinated to indium(III) via dative bonds. The average In–N bond distances for **1b** and **2b** ( $2.341$  and  $2.320$  Å, respectively) are slightly shorter than those in their *mes*-BIAN- $\text{InCl}_3$ <sup>12</sup> and dipp-TIP- $\text{InCl}_3$  counterparts ( $2.35$  and  $2.38$  Å).<sup>51</sup> The introduction of an electron-withdrawing  $\text{NO}_2$  group (in **3b**) and electron-donating  $\text{NMe}_2$  (in **4b**) and  $\text{OMe}$  groups (in **5b**) did not affect the average In–N bond distances greatly. Their average In–N bond distances ( $2.317$  Å in **3b**,  $2.324$  Å in **4b**, and  $2.331$  Å in **5b**) remained similar to those for **1b** and **2b**. Notably, complexes **1b–5b** all exhibit In–Cl bond distances significantly longer than that for  $\text{InCl}_3(\text{THF})_2$  ( $2.331(3)$  Å).<sup>61</sup> The In–Cl bond distances in **1b** and **2b** range from  $2.3643(17)$  to  $2.3897(5)$  Å and are shorter than those in the related *mes*-BIAN- $\text{InCl}_3$ , likely due to the increased electron donation from the *mes*-BIAN ligand in the latter, resulting in a weakening of the In–Cl bonds.<sup>12</sup> Although **4b** and **5b** bear ligands that are more electron-rich than those of **3b**, the average In–Cl bond distances in these complexes are similar ( $2.425$ ,  $2.423$ , and  $2.426$  Å in **3b**, **4b**, and **5b**, respectively).

**Absorption and Electrochemical Studies.** To understand the absorption profile of the indium(III) complexes, UV–vis absorption spectroscopic measurements were carried out for **1b–5b**. The absorption spectra obtained for each of the

complexes at 298 K are depicted in Figure 2. Complexes **1b–5b** typically exhibit two major sets of absorption bands. The

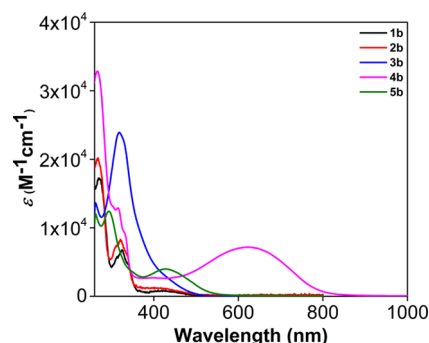


**Figure 2.** UV–vis spectra for **1b** and **2b** in THF, **3b** and **5b** in DMF, and **4b** in DCM solution. All solutions were prepared at concentrations of 0.10 mM.

bands are assigned to a mixture of the intraligand  $\pi\text{--}\pi^*$  charge transfer transitions between the arylimine and the acenaphthene motifs, according to the TD-DFT calculations (*vide infra*). The spectrum is significantly red-shifted when the electron donating  $\text{NMe}_2$  group is present on the di-(arylimino) moiety, inducing a smaller HOMO–LUMO gap due to a more destabilized HOMO. Although inductively electron-rich alkyl groups are present in **1b** and **2b** (i.e., 2,6-diisopropyl and 2,6-dimethyl), the effect is not as strong as the mesomerically donating groups in **4b** and **5b** (i.e., 4-dimethylamino and 4-methoxy). This is consistent with DFT theoretical calculations from the Zysman-Colman group, where they reported that the HOMO of the ligand is destabilized by 1.1 eV when a mesomerically electron donating ( $\text{NMe}_2$ ) group is present within the ligand backbone, whereas a destabilization of only 0.29 eV is achieved when an inductively electron-rich alkyl (2,4,6-trimethyl) group is introduced.<sup>14</sup> The single intense absorption band at ca. 320 nm in **3b** may result from a coincidental convergence of multiple intraligand charge transfer transitions.

With an initial objective to identify a suitable reducing agent with an adequate reduction potential to obtain the indium(I) counterparts of complexes **1b** to **4b**, their redox properties were examined by cyclic voltammetry. The redox potentials of accessible reduction and oxidation waves are summarized in Table 1. The voltamogram for **5b** has not been collected in this report since its redox potential is expected to be identical to the previously reported compound **6**, which has been recorded in ACN. Since the molecular structures of **5b** and **6** are solvent dependent, their redox potentials would be affected by the solvent used.<sup>50</sup> All potentials are reported relative to the ferrocenium/ferrocene ( $\text{Fc}^+/\text{Fc}$ ) redox couple. A direct comparison of the voltamograms of **1b–4b** cannot be made due to their disparate solubility properties and the differences in their coordination spheres. However, it is worth noting that the electrochemical behavior of **1b**, **2b**, and **3b** consist of four irreversible reductions and a series of oxidations (Figure 3). The irreversibility may stem from the following. First, detachment of a chloride ligand or coordination of a solvent molecule to the indium species formed during the voltammetric sweep may occur, since the reduction of the indium(III) center may involve structural changes arising from the anion dissociation. Second, the ligand itself may reduce due to its noninnocent nature. Third, the putative indium(I) intermedi-



Table 1. Electrochemical Data for 1b–4b

	potential (V vs Fc <sup>+</sup> /Fc)	
	cathodic peaks	anodic peaks
1b	−1.61	−2.72
	−1.87	−2.26
	−2.41	−1.75
	−2.95	−0.54
		+0.22
2b	−1.14	−2.57
	−1.61	−2.11
	−2.30	−1.38
	−2.84	−0.98
		−0.42
3b	−1.25	−2.14
	−1.97	−1.64
	−2.32	−1.21
	−2.49	−0.08
		+0.51
4b	+0.28	−1.47
	−0.06	−1.15
	−1.24	−0.72
	−1.62	+0.44
	−1.85	+0.64

ates formed at the electrode surface may disproportionate, which is also supported by the experimental findings (*vide infra*). In contrast, the electrochemical behavior of 4b in DCM showed a chemically reversible reduction wave at −1.20 V on the time scale of the experiment (Figure 3d). The reversibility of the first reduction wave observed in 4b suggested an increased stability of the transient [(NMe<sub>2</sub>Ar-BIAN)InCl<sub>3</sub>]<sup>−</sup>

complex due to the stronger electron donation from 4a to the metal center, thus preventing dissociation of the Ar-BIAN ligand upon reduction. This is consistent with our previous observations on the voltammogram recorded for 6 bearing electron donating −OMe groups. Compound 6 also showed an electrochemically reversible reduction wave at −1.46 V, which was attributed to the stronger electron donation from the corresponding −OMe substituted ligand to the indium(III) center.<sup>50</sup> Although the assignment of each reduction and oxidation processes in 1b–4b was hampered by the complex processes at the electrode surface, the redox behaviors of 1b–4b indicate that mild reducing agents with potentials between −1.0 and −2.0 V can be utilized to effect reduction of the In(III) complexes.<sup>62</sup>

In view of this, the reduction of 1b using magnesium anthracene was attempted in THF. Interestingly, based on the <sup>1</sup>H NMR spectra and visual observations of the reaction mixture, reduction of the Ar-BIAN ligand and the indium(III) nucleus appeared to occur concurrently. Indium metal deposition was observed from the reaction mixture, and the protonated reduced Ar-BIAN ligand was the only isolated reaction product as indicated by a singlet at 5.06 ppm (Figure S11). This chemical shift corresponds to the two N–H bonds of a reduced Ar-BIAN ligand, which matches the spectrum obtained from an independent reduction of ligand 1a. Similarly, reduction reactions of 6 using CoCp<sub>2</sub> resulted in formation of the reduced Ar-BIAN ligand MeOAr-BIAN-H<sub>2</sub> (8). The presence of 8 was confirmed by <sup>1</sup>H NMR spectroscopy<sup>63</sup> and single-crystal X-ray diffraction (Figure S12). The observed formation of the reduced ligand in the attempted reduction reactions of 1b and 6 may be attributed to the redox noninnocence of the Ar-BIAN ligands. As mentioned in the Introduction, it has been demonstrated that reduction reactions sometimes occur on the diimine ligand rather than the metal center among both main group<sup>64,65</sup> and transition metal

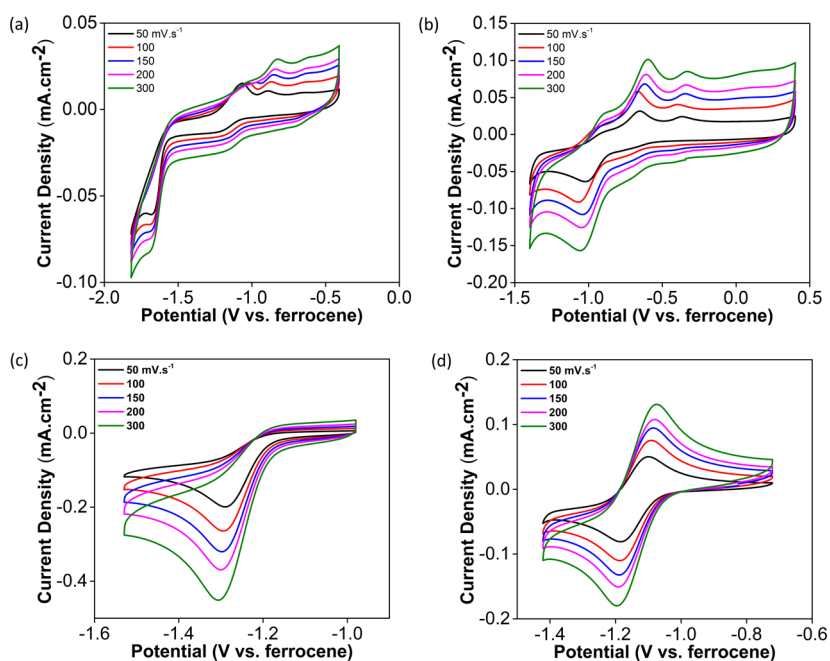


**Figure 3.** Cyclic voltammograms of the first reduction wave for 1b (a) in THF, 2b (b) in THF, 3b (c) in DMF, and 4b (d) in DCM solution at 298 K with 0.10 M (nBu<sub>4</sub>N)PF<sub>6</sub> as the supporting electrolyte and glassy carbon (3 mm in diameter) as the working electrode. Data were collected using scan rates ranging from 50 to 300 mV s<sup>−1</sup>, and all potentials reported were referenced to Fc<sup>+</sup>/Fc.

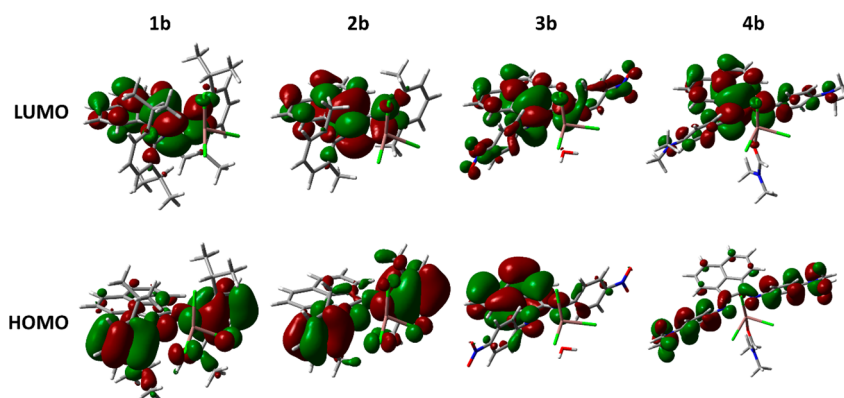


Figure 4. Electron density distributions of the frontier orbitals for 1b–4b.

complexes.<sup>1,66</sup> Future studies will involve the use of (i) bulkier aryl substituents to kinetically stabilize the indium(I) products, which has been successfully adopted for indium(I) complexes comprising redox innocent ligands;<sup>67</sup> (ii) more electron-rich aryl substituents to preclude electron transfer from the indium(I) center to the Ar-BIAN ligand; and (iii) ligands and solvents of different electronic properties to stabilize the heteroleptic indium(I) center. Studies involving these approaches are currently undergoing.

**Computational Studies.** DFT and TD-DFT calculations were undertaken to predict the electronic absorption spectra of the complexes described herein. The geometry of each complex was optimized with the hybrid functional B3LYP/6-31+G\*, using the pseudo potential LANL2DZ basis set for the indium and chlorine atoms. A larger basis set 6-31++G\* was used for our previously reported complexes 6 and 7, with almost identical outcomes as those obtained from the basis set 6-31+G\*. Hence, all geometry optimizations were carried out with the smaller 6-31+G\* basis set in this article since it would be computationally cheaper. The optimized ground state structures for all complexes agreed closely with our X-ray crystallographic studies. Each optimized structure of 1b and 2b displays a plane of symmetry bisecting the acenaphthene and indium metal center. The frontier orbitals illustrating the electron density distribution for 1b–4b are shown in Figure 4. For 1b, 2b, and 4b, the HOMO is mostly distributed on the di(arylimine) part of the Ar-BIAN ligand, while the LUMO is mainly localized on the acenaphthene moiety. However, for 3b, the HOMO is localized on the acenaphthene bay region, whereas the LUMO has distributed contributions throughout the entire ligand. This intriguing reversal in orbital density when strongly electron-withdrawing groups are installed on the di(arylimine) motif is consistent with previous DFT calculations performed on a series of Ar-BIAN ligand by Zysman-Colman and co-workers.<sup>14</sup> From the TD-DFT analysis, the absorption maxima in 1b and 2b ( $\lambda_{\text{max}} = 320$  nm) are mainly attributed to electronic transitions from the HOMO–3  $\rightarrow$  LUMO+1, while for 3b ( $\lambda_{\text{max}} = 318$  nm), it corresponds largely to a combination of the HOMO  $\rightarrow$  LUMO+3, HOMO–1  $\rightarrow$  LUMO+2, and HOMO–8  $\rightarrow$  LUMO transition (Tables S32–S34). In the case of 4b, the calculated predominant contribution to the lower energy absorption maximum ( $\lambda_{\text{max}} = 630$  nm) corresponds exclusively to the HOMO  $\rightarrow$  LUMO transition, whereas the higher energy UV absorption band ( $\lambda_{\text{max}} = 267$  nm) consists of a combination of contributions from HOMO–14  $\rightarrow$  LUMO, HOMO–15  $\rightarrow$  LUMO, and HOMO  $\rightarrow$  LUMO+7 transitions (Table S35).

## CONCLUSIONS

We have conducted a comprehensive investigation on the synthesis, absorption, and electrochemical properties of a series of five indium(III) complexes bearing redox noninnocent Ar-BIAN ligands. All the complexes within this study absorb light over wavelengths ranging from 380–800 nm, with 4b absorbing furthest to the red region, which can be attributed to the small HOMO–LUMO gap due to the  $-\text{NMe}_2$  substituent. On the other hand, the absorption spectrum of 3b revealed a single intense band at 320 nm resulting from enlarged frontier orbital energy gaps arising from the electron-withdrawing  $-\text{NO}_2$  group. The CVs showed irreversible reduction waves ranging from  $-1.2$  to  $-1.9$  V for compounds 1b–3b, whereas this reduction was observed to be chemically reversible for compound 4b and our previously reported complex 6. Although disproportionation and ligand reduction were observed during our attempted reduction of 1b and 6, we ascribe it to the noninnocent behavior of the Ar-BIAN ligand, which can accommodate the extra electrons more readily than the In metal center. Future work will involve modifying both the steric and electronic properties of the Ar-BIAN ligands, as well as using different counteranions and ligands in heteroleptic systems to prevent electron transfer from the metal to the Ar-BIAN ligand.

## EXPERIMENTAL DETAILS

**General Procedures.** All reactions with  $\text{InCl}_3$  and the recrystallization of products were performed under dry and inert atmospheres by using a combination of standard Schlenk line techniques and a Vacuum Atmospheres Company  $\text{N}_2$  glovebox. Solvents including tetrahydrofuran (THF), diethyl ether ( $\text{Et}_2\text{O}$ ), and pentane were distilled over Na/benzophenone and degassed using freeze–pump–thaw cycles prior to use. Anhydrous acetonitrile (ACN) was collected from a PURE SOLV MD-5 solvent purification system and stored in a glovebox. Anhydrous 1,2-dimethoxyethane (DME) and dichloromethane (DCM) were distilled over calcium hydride ( $\text{CaH}_2$ ) and stored in a glovebox. Anhydrous  $N,N$ -dimethylformamide (DMF) in a Sure-Seal bottle was purchased from Sigma-Aldrich and used as received. Deuterated chloroform ( $\text{CDCl}_3$ ) and acetonitrile ( $\text{CD}_3\text{CN}$ ) were distilled over  $\text{CaH}_2$  and stored over 4 Å molecular sieves. Deuterated acetone was distilled over potassium carbonate ( $\text{K}_2\text{CO}_3$ ). All reagents were purchased from commercial sources and were used without further purification. Synthetic procedures for 6 and 7 were reported by our team previously.<sup>50</sup> The  $^1\text{H}$  and  $^{13}\text{C}\{^1\text{H}\}$  NMR spectra were recorded at 298 K on Bruker AV400 and BBFO 400 spectrometers. The chemical shift values are reported in parts per million (ppm) relative to TMS, using residual protonated solvents as the internal standards ( $^1\text{H}$ :  $\delta = 7.26$  for  $\text{CDCl}_3$  and  $\delta = 1.94$  for  $\text{CD}_3\text{CN}$ ;  $^{13}\text{C}$ :  $\delta = 77.2$  for  $\text{CDCl}_3$  and  $\delta = 118.3$  for  $\text{CD}_3\text{CN}$ ). The

<sup>115</sup>In NMR data have not been reported due to the large quadrupolar moments of the nuclei, which result in broad and essentially unobservable NMR signals in the solid-state.<sup>68–70</sup> This is especially the case due to the low symmetry of our reported complexes.

**Other Instrumentation.** High-resolution mass spectra were obtained by using a Waters Q-ToF Premier, with ESI mode. Crystallographic data were recorded on a Bruker X8 CCD diffractometer. UV–vis spectroscopic measurements were performed using a Shimadzu UV-3600 UV–vis–NIR spectrophotometer. Cyclic voltammetry (CV) experiments were conducted in a glovebox with N<sub>2</sub> atmosphere, using a Biologic SP-300 potentiostat with 1.0 mM solutions of each sample and 0.10 M of tetrabutylammonium hexafluorophosphate (*n*-Bu<sub>4</sub>NPF<sub>6</sub>) as the electrolyte. Melting points were measured on an OptiMelt automated melting pointing system using sealed glass capillaries under argon and were uncorrected.

**Synthesis of Indium(III) Complexes.** (*dipp*-BIAN)/InCl<sub>3</sub> (**1b**). A solution of InCl<sub>3</sub> (0.025 g, 0.11 mmol) in THF (5 mL) was added to a solution of *dipp*-BIAN (0.056 g, 0.11 mmol) in THF (5 mL) at room temperature. (See [Supporting Information](#) for synthesis of *dipp*-BIAN.) The resulting orange solution was stirred overnight, after which all volatiles were removed under vacuum. The resultant orange powder was recrystallized by vapor diffusion of pentane into a DME solution of the crude product, and the isolated yield was 0.061 g (76%). <sup>1</sup>H NMR (400 MHz, CDCl<sub>3</sub>): δ = 0.87 (d, *J* = 7.2 Hz, 12 H), 1.38 (d, *J* = 6.8 Hz, 12 H), 3.07 (sept, *J* = 6.8 Hz, 4 H), 6.75 (d, *J* = 7.2 Hz, 2 H), 7.40 (d, *J* = 7.6 Hz, 4 H), 7.50–7.54 (m, 2 H), 7.60 (t, *J* = 8.0 Hz, 2 H), 8.17 (d, *J* = 8.0 Hz, 2 H). <sup>13</sup>C{<sup>1</sup>H} NMR (100 MHz, CDCl<sub>3</sub>): δ = 24.4, 24.8, 29.9, 125.1, 126.2, 127.8, 129.1, 129.3, 131.1, 133.2, 140.0, 140.3, 144.3, 162.7. M.p.: decomposed at 280 °C. HRMS (ESI+, *m/z*) calcd for C<sub>36</sub>H<sub>40</sub>N<sub>2</sub>InCl<sub>3</sub>Na [M + Na]<sup>+</sup> *m/z* = 743.1194, found 743.1179. Anal. Calcd for C<sub>36</sub>H<sub>40</sub>N<sub>2</sub>InCl<sub>3</sub>: C, 59.90; H, 5.59; N, 3.88. Found: C, 59.56; H, 5.43; N, 3.82.

(2,6-Me<sub>2</sub>Ar-BIAN)/InCl<sub>3</sub> (**2b**). The procedure was identical to the one reported above for **1b**. The following quantities of reagents were used: InCl<sub>3</sub> (0.023 g, 0.10 mmol) in THF (5 mL), 2,6-Me<sub>2</sub>Ar-BIAN (0.040 g, 0.10 mmol) in THF (5 mL). (zsee [Supporting Information](#) for synthesis of 2,6-Me<sub>2</sub>Ar-BIAN.) Orange block-like crystals suitable for single-crystal X-ray analysis were obtained by recrystallization via vapor diffusion of pentane into a THF solution of the crude product, and the isolated yield was 0.026 g (41%). <sup>1</sup>H NMR (400 MHz, CDCl<sub>3</sub>): δ = 2.30 (s, 12 H), 6.79 (d, *J* = 7.2 Hz, 2 H), 7.28–7.30 (m, 4 H), 7.33–7.37 (m, 2 H), 7.62 (t, *J* = 7.8 Hz, 2 H), 8.21 (d, *J* = 8.4 Hz, 2 H). <sup>13</sup>C{<sup>1</sup>H} NMR (100 MHz, CDCl<sub>3</sub>): δ = 19.0, 125.8, 126.7, 128.4, 129.6 (two overlapping signals), 129.9, 131.1, 133.5, 142.1, 144.6, 162.3. M.p.: decomposed at 273 °C. HRMS (ESI+, *m/z*) calcd for C<sub>28</sub>H<sub>24</sub>N<sub>2</sub>InCl<sub>3</sub>Na [M + Na]<sup>+</sup> *m/z* = 630.9942, found 630.9954. Anal. Calcd for C<sub>28</sub>H<sub>24</sub>N<sub>2</sub>InCl<sub>3</sub>·THF·H<sub>2</sub>O: C, 54.92; H, 4.90; N, 4.00. Found: C, 55.16; H, 4.93; N, 4.26.

(*p*-NO<sub>2</sub>Ar-BIAN)/InCl<sub>3</sub> (**3b**). The procedure was similar to the one reported above for complex **1b** except that this reaction was carried out under reflux conditions overnight. The following quantities of compounds were used: InCl<sub>3</sub> (0.044 g, 0.20 mmol) and *p*-NO<sub>2</sub>Ar-BIAN (0.084 g, 0.20 mmol) in THF (7 mL). (See [Supporting Information](#) for synthesis of *p*-NO<sub>2</sub>Ar-BIAN.) The resultant yellow solid was purified by washing with THF, and the isolated yield was 0.083 g (64%). The purity of the product was confirmed by elemental analysis. Yellow block-like crystals suitable for single-crystal X-ray analysis were obtained by recrystallization from an ACN solution of the crude product. <sup>1</sup>H NMR (400 MHz, acetone-*d*<sub>6</sub>): δ = 7.27 (d, *J* = 6.8 Hz, 2 H), 7.75–7.79 (m, 6 H), 8.44 (d, *J* = 8.4 Hz, 2 H), 8.55–8.58 (m, 4 H). The <sup>13</sup>C{<sup>1</sup>H} NMR could not be obtained due to the poor solubility of **3b** in most of the available deuterated solvents. M.p.: decomposed after 320 °C. HRMS (ESI+, *m/z*) calcd for C<sub>24</sub>H<sub>14</sub>Cl<sub>3</sub>InN<sub>4</sub>O<sub>4</sub>Na [M + Na]<sup>+</sup> *m/z* = 664.9017, found 664.9005. Anal. Calcd for C<sub>24</sub>H<sub>14</sub>Cl<sub>3</sub>InN<sub>4</sub>O<sub>4</sub>·THF: C, 46.99; H, 3.10; N, 7.83. Found: C, 46.63; H, 3.45; N, 8.15.

(*p*-NMe<sub>2</sub>Ar-BIAN)/InCl<sub>3</sub> (**4b**). The procedure was identical to the one reported above for **1b**. The following quantities of reagents were used: InCl<sub>3</sub> (0.066 g, 0.30 mmol) in THF (5 mL) and *p*-NMe<sub>2</sub>Ar-BIAN (0.130 g, 0.30 mmol) in THF (5 mL). (See [Supporting Information](#)

for synthesis of *p*-NMe<sub>2</sub>Ar-BIAN.) The purple solution was stirred overnight, after which all volatiles were removed under vacuum. The resultant deep blue solid was washed with Et<sub>2</sub>O. Purple needle-like crystals suitable for single-crystal X-ray analysis were obtained from recrystallization by vapor diffusion of Et<sub>2</sub>O into a DMF solution of the crude product, and the isolated yield was 0.13 g (68%). <sup>1</sup>H NMR (400 MHz, CD<sub>2</sub>Cl<sub>2</sub>, 25 °C, *fac*-isomer): δ = 3.09 (s, broad, 12 H), 6.88 (d, *J* = 9.2, 2 H), 7.04–7.06 (m, 4 H), 7.40 (d, *J* = 6.8, 2 H), 7.54–7.60 (m, 4 H), 8.17 (d, *J* = 8.0 Hz, 2 H). <sup>13</sup>C{<sup>1</sup>H} NMR (100 MHz, CD<sub>2</sub>Cl<sub>2</sub>): δ = 40.6, 40.7, 112.5, 123.0 (broad, may have peaks overlapping), 124.3, 126.1 (broad, may have peaks overlapping), 127.2, 128.8, 129.1, 131.3 (two peaks), 131.7, 132.8 (broad, may have peaks overlapping), 133.5, 143.8, 144.1, 150.9, 151.3 (broad, may have peaks overlapping), 157.7. M.p.: 198–202 °C. HRMS (ESI+, *m/z*) calcd for C<sub>31</sub>H<sub>33</sub>N<sub>3</sub>OInCl<sub>3</sub>Na [M + Na]<sup>+</sup> *m/z* = 734.0687, found 734.0652. Anal. Calcd for C<sub>31</sub>H<sub>33</sub>N<sub>3</sub>OInCl<sub>3</sub>·H<sub>2</sub>O: C, 50.95; H, 4.83; N, 9.58. Found: C, 50.90; H, 4.90; N, 9.32.

(*p*-MeOAr-BIAN)/InCl<sub>3</sub>·DMF (**5b**).<sup>50</sup> The synthetic procedure was reported in a recent publication by our team and has been included here for completeness. Recrystallization by vapor diffusion of Et<sub>2</sub>O into a DMF solution of the red solid resulted in samples suitable for single-crystal X-ray analysis. <sup>1</sup>H NMR (400 MHz, CD<sub>3</sub>CN, *fac*-isomer): δ = 3.92 (s, 6 H), 7.16–7.18 (m, 4 H), 7.33–7.36 (m, 4 H), 7.56–7.65 (m, 4 H), 8.31 (d, *J* = 6.8 Hz, 2 H). <sup>13</sup>C{<sup>1</sup>H} NMR (100 MHz, DMF-*d*<sub>7</sub>): δ = 56.4, 114.4, 115.8, 116.0, 119.9, 120.4 (broad overlapping peaks), 122.8, 124.3 (broad overlapping peaks), 124.6, 127.2 (broad overlapping peaks), 129.0 (broad overlapping peaks), 130.1, 130.3, 133.5, 138.7, 158.1, 160.6. HRMS (ESI+, *m/z*) calcd for C<sub>29</sub>H<sub>27</sub>Cl<sub>3</sub>InN<sub>3</sub>O<sub>3</sub>Na [M + Na]<sup>+</sup> *m/z* = 708.0054, found 708.0081. Anal. Calcd for C<sub>29</sub>H<sub>27</sub>N<sub>3</sub>O<sub>3</sub>InCl<sub>3</sub>·H<sub>2</sub>O: C, 49.43; H, 4.15; N, 5.96. Found: C, 49.84; H, 4.55; N, 6.12.

**Reduction of [(*p*-MeOAr-BIAN)<sub>2</sub>InCl<sub>2</sub>]<sup>+</sup>[InCl<sub>4</sub>]<sup>−</sup> (**6**).** A THF solution (5 mL) of CoCp<sub>2</sub> was added dropwise to a THF suspension (5 mL) of **6** at room temperature. The resulting brown suspension was stirred for 2 h, after which all volatiles were removed under vacuum. The crude purple solid was washed with Et<sub>2</sub>O, and the purple filtrate was filtered and concentrated. The <sup>1</sup>H NMR experiments were conducted on the resultant purple solid. <sup>1</sup>H NMR (400 MHz, C<sub>6</sub>D<sub>6</sub>): 3.33 (s, 6 H), 4.93 (s, 2 H), 6.72–6.77 (m, 8 H), 7.12–7.42 (m, overlapping with signal from C<sub>6</sub>D<sub>6</sub>), 7.43 (d, *J* = 8.0 Hz, 2 H).

**Theoretical Basis.** DFT calculations were used to evaluate both the geometries and energies of the different indium complexes possessing one or two coordinated Ar-BIAN ligands. The initial energy and geometry optimization was carried out at the B3LYP<sup>71–73</sup> level with the 6-31+G\* basis set for nonmetal atoms,<sup>74</sup> together with the pseudopotential LANL2DZ<sup>75</sup> for the In and Cl atoms. The agreement between the experimentally determined and the computed structures supports the method used. Frequency calculations were carried out at this level to confirm that a minimum had been achieved. To account for solvent effects, a reaction field calculation with radii and nonelectrostatic terms and the SMD solvation model was used.<sup>76</sup> All the TD-DFT calculations were carried out using the Gaussian 09 program package.<sup>71–73,77</sup>

## ■ ASSOCIATED CONTENT

### ● Supporting Information

The Supporting Information is available free of charge on the ACS Publications website at DOI: 10.1021/acs.inorgchem.7b00539.

General procedures, experimental details, photophysical and electrochemical characterization protocols, <sup>1</sup>H and <sup>13</sup>C NMR spectra, crystallographic data, and computational details (PDF)

### Accession Codes

CCDC 1535077–1535081 contain the supplementary crystallographic data for this paper. These data can be obtained free of charge via [www.ccdc.cam.ac.uk/data\\_request/cif](http://www.ccdc.cam.ac.uk/data_request/cif), or by email-



ing [data\\_request@ccdc.cam.ac.uk](mailto:data_request@ccdc.cam.ac.uk), or by contacting The Cambridge Crystallographic Data Centre, 12 Union Road, Cambridge CB2 1EZ, UK; fax: +44 1223 336033.

## AUTHOR INFORMATION

### Corresponding Authors

\*E-mail: [jdal@unex.es](mailto:jdal@unex.es).

\*E-mail: [hansen@ntu.edu.sg](mailto:hansen@ntu.edu.sg).

\*E-mail: [fgarcia@ntu.edu.sg](mailto:fgarcia@ntu.edu.sg).

### ORCID

Han Sen Soo: 0000-0001-6502-2313

Felipe García: 0000-0002-9605-3611

### Notes

The authors declare no competing financial interest.

## ACKNOWLEDGMENTS

The authors also gratefully acknowledge the Agency for Science, Technology and Research (A\*STAR), AME IRG grant A1783c0003 for funding this research. FGG is also supported by NTU start-up grant (M4080552) and MOE Tier 1 grant (M4011441) for financial support. H.S.S. is supported by a NTU start-up grant (M4081012), MOE Tier 1 grants (M4011144 and M4011611), and the Nanyang Assistant Professorship (M4081154). H.S.S. also thanks the support from the Solar Fuels Laboratory at NTU and the Singapore-Berkeley Research Initiative for Sustainable Energy (SinBeR-ISE) CREATE Program. J.D. thanks the Fundación Computación y Tecnologías Avanzadas de Extremadura (COMPUTAEX) for computing resources.

## REFERENCES

- (1) Butin, K. P.; Beloglazkina, E. K.; Zyk, N. V. Metal complexes with non-innocent ligands. *Russ. Chem. Rev.* **2005**, *74*, 531.
- (2) Lyaskovskyy, V.; de Bruin, B. Redox Non-Innocent Ligands: Versatile New Tools to Control Catalytic Reactions. *ACS Catal.* **2012**, *2*, 270–279.
- (3) Jørgensen, C. K. Differences between the four halide ligands, and discussion remarks on trigonal-bipyramidal complexes, on oxidation states, and on diagonal elements of one-electron energy. *Coord. Chem. Rev.* **1966**, *1*, 164–178.
- (4) Chirik, P. J.; Wieghardt, K. Radical Ligands Confer Nobility on Base-Metal Catalysts. *Science* **2010**, *327*, 794–795.
- (5) Matei, I.; Lixandru, T. *Bul. Inst. Politeh. Iasi* **1967**, *13*, 245–255.
- (6) Kern, T.; Monkowius, U.; Zabel, M.; Knör, G. Mononuclear Copper(I) Complexes Containing Redox-Active 1,2-Bis(aryl-imino)-acenaphthene Acceptor Ligands: Synthesis, Crystal Structures and Tuneable Electronic Properties. *Eur. J. Inorg. Chem.* **2010**, *2010*, 4148–4156.
- (7) Li, L.; Lopes, P. S.; Rosa, V.; Figueira, C. A.; Lemos, M. A. N. D. A.; Duarte, M. T.; Aviles, T.; Gomes, P. T. Synthesis and structural characterisation of (aryl-BIAN)copper(I) complexes and their application as catalysts for the cycloaddition of azides and alkynes. *Dalton Trans.* **2012**, *41*, 5144–5154.
- (8) Li, L.; Lopes, P. S.; Figueira, C. A.; Gomes, C. S. B.; Duarte, M. T.; Rosa, V.; Flidel, C.; Aviles, T.; Gomes, P. T. Cationic and Neutral (Ar-BIAN)Copper(I) Complexes Containing Phosphane and Arsane Ancillary Ligands: Synthesis, Molecular Structure and Catalytic Behaviour in Cycloaddition Reactions of Azides and Alkynes. *Eur. J. Inorg. Chem.* **2013**, *2013*, 1404–1417.
- (9) Papanikolaou, P.; Akrivos, P. D.; Czapik, A.; Wicher, B.; Gdaniec, M.; Tkachenko, N. Homoleptic Bis(aryl)-acenaphthenequinonediimine–CuI Complexes – Synthesis and Characterization of a Family of Compounds with Improved Light-Gathering Characteristics. *Eur. J. Inorg. Chem.* **2013**, *2013*, 2418–2431.
- (10) Papanikolaou, P. A.; Tkachenko, N. V. Probing the excited state dynamics of a new family of Cu(I)-complexes with an enhanced light absorption capacity: excitation-wavelength dependent population of states through branching. *Phys. Chem. Chem. Phys.* **2013**, *15*, 13128–13136.
- (11) Hill, N. J.; Vargas-Baca, I.; Cowley, A. H. Recent developments in the coordination chemistry of bis(imino)acenaphthene (BIAN) ligands with s- and p-block elements. *Dalton Trans.* **2009**, 240–253.
- (12) Hill, N. J.; Reeske, G.; Moore, J. A.; Cowley, A. H. Complexes of 1,2-bis(aryl-imino)acenaphthene (Ar-BIAN) ligands with some heavy p-block elements. *Dalton Trans.* **2006**, 4838–4844.
- (13) Gasperini, M.; Ragaini, F.; Gazzola, E.; Caselli, A.; Macchi, P. Synthesis of mixed Ar,Ar'-BIAN ligands (Ar,Ar'-BIAN = bis(aryl)-acenaphthenequinonediimine). Measurement of the coordination strength of hemilabile ligands with respect to their symmetric counterparts. *Dalton Trans.* **2004**, 3376–3382.
- (14) Hasan, K.; Zysman-Colman, E. Synthesis, UV–Vis and CV properties of a structurally related series of bis(Arylimino)-acenaphthenes (Ar-BIANs). *J. Phys. Org. Chem.* **2013**, *26*, 274–279.
- (15) El-Ayaan, U.; Paulovicova, A.; Yamada, S.; Fukuda, Y. The Crystal Structure of Bis[N-(2,6-diisopropylphenyl)imino] Acenaphthene and Studies of its Copper(I) and Copper(II) Complexes. *J. Coord. Chem.* **2003**, *56*, 373–381.
- (16) Kee, J. W.; Ng, Y. Y.; Kulkarni, S. A.; Muduli, S. K.; Xu, K.; Ganguly, R.; Lu, Y.; Hirao, H.; Soo, H. S. Development of bis(arylimino)acenaphthene (BIAN) copper complexes as visible light harvesters for potential photovoltaic applications. *Inorg. Chem. Front.* **2016**, *3*, 651–662.
- (17) Fedushkin, I. L.; Skatova, A. A.; Chudakova, V. A.; Fukin, G. K.; Dechert, S.; Schumann, H. Monomeric Magnesium and Calcium Complexes Containing the Bidentate, Dianionic 1,2-Bis[(2,6-diisopropylphenyl)imino]acenaphthene Ligand. *Eur. J. Inorg. Chem.* **2003**, *2003*, 3336–3346.
- (18) Fedushkin, I. L.; Skatova, A. A.; Cherkasov, V. K.; Chudakova, V. A.; Dechert, S.; Hummert, M.; Schumann, H. Reduction of Benzophenone and 9(10H)-Anthracenone with the Magnesium Complex [(2,6-iPr<sub>2</sub>C<sub>6</sub>H<sub>3</sub>-Bian)Mg(thf)<sub>3</sub>]. *Chem. - Eur. J.* **2003**, *9*, 5778–5783.
- (19) Fedushkin, I. L.; Skatova, A. A.; Chudakova, V. A.; Fukin, G. K. Four-Step Reduction of dpp-Bian with Sodium Metal: Crystal Structures of the Sodium Salts of the Mono-, Di-, Tri- and Tetraanions of dpp-Bian. *Angew. Chem., Int. Ed.* **2003**, *42*, 3294–3298.
- (20) Johnson, L. K.; Killian, C. M.; Brookhart, M. New Pd(II)- and Ni(II)-Based Catalysts for Polymerization of Ethylene and  $\alpha$ -Olefins. *J. Am. Chem. Soc.* **1995**, *117*, 6414–6415.
- (21) Mecking, S.; Johnson, L. K.; Wang, L.; Brookhart, M. Mechanistic Studies of the Palladium-Catalyzed Copolymerization of Ethylene and  $\alpha$ -Olefins with Methyl Acrylate. *J. Am. Chem. Soc.* **1998**, *120*, 888–899.
- (22) Svejda, S. A.; Johnson, L. K.; Brookhart, M. Low-Temperature Spectroscopic Observation of Chain Growth and Migratory Insertion Barriers in ( $\alpha$ -Diimine)Ni(II) Olefin Polymerization Catalysts. *J. Am. Chem. Soc.* **1999**, *121*, 10634–10635.
- (23) Tempel, D. J.; Johnson, L. K.; Huff, R. L.; White, P. S.; Brookhart, M. Mechanistic Studies of Pd(II)- $\alpha$ -Diimine-Catalyzed Olefin Polymerizations I. *J. Am. Chem. Soc.* **2000**, *122*, 6686–6700.
- (24) Ittel, S. D.; Johnson, L. K.; Brookhart, M. Late-Metal Catalysts for Ethylene Homo- and Copolymerization. *Chem. Rev.* **2000**, *100*, 1169–1204.
- (25) Shultz, L. H.; Brookhart, M. Measurement of the Barrier to  $\beta$ -Hydride Elimination in a  $\beta$ -Agostic Palladium–Ethyl Complex: A Model for the Energetics of Chain-Walking in ( $\alpha$ -Diimine)PdR<sup>+</sup> Olefin Polymerization Catalysts. *Organometallics* **2001**, *20*, 3975–3982.
- (26) Leatherman, M. D.; Svejda, S. A.; Johnson, L. K.; Brookhart, M. Mechanistic Studies of Nickel(II) Alkyl Agostic Cations and Alkyl Ethylene Complexes: Investigations of Chain Propagation and Isomerization in ( $\alpha$ -diimine)Ni(II)-Catalyzed Ethylene Polymerization. *J. Am. Chem. Soc.* **2003**, *125*, 3068–3081.



- (27) Liu, W.; Brookhart, M. Mechanistic Studies of Palladium(II)- $\alpha$ -Diimine-Catalyzed Polymerizations of cis- and trans-2-Butenes. *Organometallics* **2004**, *23*, 6099–6107.
- (28) Fliedel, C.; Rosa, V.; Santos, C. I. M.; Gonzalez, P. J.; Almeida, R. M.; Gomes, C. S. B.; Gomes, P. T.; Lemos, M. A. N. D. A.; Aullon, G.; Welter, R.; Aviles, T. Copper(II) complexes of bis(aryl-imino)acenaphthene ligands: synthesis, structure, DFT studies and evaluation in reverse ATRP of styrene. *Dalton Trans.* **2014**, *43*, 13041–13054.
- (29) Fedushkin, I. L.; Skatova, A. A.; Chudakova, V. A.; Cherkasov, V. K.; Fukin, G. K.; Lopatin, M. A. Reduction of 1,2-Bis[(2,6-diisopropylphenyl)imino]acenaphthene (dpp-Bian) with Alkali Metals – A Study of the Solution Behaviour of (dpp-Bian)<sup>n-</sup>[M<sup>+</sup>]<sub>n</sub> (M = Li, Na; n = 1–4) with UV/Vis, ESR and <sup>1</sup>H NMR Spectroscopy. *Eur. J. Inorg. Chem.* **2004**, *2004*, 388–393.
- (30) Fedushkin, I. L.; Chudakova, V. A.; Skatova, A. A.; Fukin, G. K. Solvent-free alkali and alkaline earth metal complexes of di-imine ligands. *Heteroat. Chem.* **2005**, *16*, 663–670.
- (31) Fedushkin, I. L.; Chudakova, V. A.; Skatova, A. A.; Fukin, G. K. Solvent-free alkali and alkaline earth metal complexes of di-imine ligands. *Heteroat. Chem.* **2006**, *17*, 618–618.
- (32) Fedushkin, I. L.; Skatova, A. A.; Chudakova, V. A.; Cherkasov, V. K.; Dechert, S.; Schumann, H. Magnesium and calcium complexes with two diimine radical-anion ligands. Molecular structure of the Ca complex with 1,2-bis[(2,6-diisopropylphenyl)imino]acenaphthene. *Russ. Chem. Bull.* **2004**, *53*, 2142–2147.
- (33) Fedushkin, I. L.; Khvoinova, N. M.; Skatova, A. A.; Fukin, G. K. Oxidative Addition of Phenylacetylene through C-H Bond Cleavage To Form the Mg<sup>II</sup>-dpp-Bian Complex: Molecular Structure of [Mg{dpp-Bian(H)}(CCPh)(thf)<sub>2</sub>] and Its Diphenylketone Insertion Product [Mg(dpp-Bian)<sup>-</sup>{OC(Ph)<sub>2</sub>CCPh}(thf)]. *Angew. Chem., Int. Ed.* **2003**, *42*, 5223–5226.
- (34) Fedushkin, I. L.; Chudakova, V. A.; Fukin, G. K.; Dechert, S.; Hummert, M.; Schumann, H. Protonation of magnesium and sodium complexes containing dianionic diimine ligands. Molecular structures of 1,2-bis[(2,6-diisopropylphenyl)imino]acenaphthene (dpp-BIAN), [(dpp-BIAN)H<sub>2</sub>(Et<sub>2</sub>O)], and [(dpp-BIAN)HNa(Et<sub>2</sub>O)]. *Russ. Chem. Bull.* **2004**, *53*, 2744–2750.
- (35) Fedushkin, I. L.; Skatova, A. A.; Lukoyanov, A. N.; Chudakova, V. A.; Dechert, S.; Hummert, M.; Schumann, H. Reactions of (dpp-BIAN)Mg(thf)<sub>3</sub> complex (dpp-BIAN is 1,2-bis[(2,6-diisopropylphenyl)imino]acenaphthene) with halogen-containing reagents. *Russ. Chem. Bull.* **2004**, *53*, 2751–2762.
- (36) Fedushkin, I. L.; Skatova, A. A.; Chudakova, V. A.; Khvoinova, N. M.; Baurin, A. Y.; Dechert, S.; Hummert, M.; Schumann, H. Stable Gernylenes Derived from 1,2-Bis(arylimino)acenaphthenes. *Organometallics* **2004**, *23*, 3714–3718.
- (37) Fedushkin, I. L.; Khvoinova, N. M.; Baurin, A. Y.; Fukin, G. K.; Cherkasov, V. K.; Bubnov, M. P. Divalent Germanium Compound with a Radical-Anionic Ligand: Molecular Structures of (dpp-BIAN)<sup>•-</sup>GeCl and Its Hydrochloration Products [(dpp-BIAN)-(H)<sub>2</sub>]<sup>•+</sup>[GeCl<sub>3</sub>]<sup>-</sup> and [(dpp-BIAN)(H)<sub>2</sub>]<sup>•+</sup>[GeCl<sub>3</sub>]<sup>-</sup> (dpp-BIAN = 1,2-Bis[(2,6-diisopropylphenyl)imino]acenaphthene. *Inorg. Chem.* **2004**, *43*, 7807–7815.
- (38) Fedushkin, I. L.; Khvoinova, N. M.; Baurin, A. Y.; Chudakova, V. A.; Skatova, A. A.; Cherkasov, V. K.; Fukin, G. K.; Baranov, E. V. Reactions of germanium(II), tin(II), and antimony(III) chlorides with acenaphthene-1,2-diimines. *Russ. Chem. Bull.* **2006**, *55*, 74–83.
- (39) Hill, N. J.; Vasudevan, K.; Cowley, A. H. *Jordan J. Chem.* **2006**, *1*, 47–54.
- (40) Reeske, G.; Hoberg, C. R.; Hill, N. J.; Cowley, A. H. Capture of Phosphorus(I) and Arsenic(I) Moieties by a 1,2-Bis(arylimino)-acenaphthene (Aryl-BIAN) Ligand. A Case of Intramolecular Charge Transfer. *J. Am. Chem. Soc.* **2006**, *128*, 2800–2801.
- (41) Reeske, G.; Cowley, A. H. Direct reactions of tellurium tetrahalides with chelating nitrogen ligands. Trapping of TeI<sub>2</sub> by a 1,2-bis(arylimino)acenaphthene (aryl-BIAN) ligand and C-H activation of an  $\alpha,\alpha'$ -diiminopyridine (DIMPY) ligand. *Chem. Commun.* **2006**, 4856–4858.
- (42) Dutton, J. L.; Farrar, G. J.; Sgro, M. J.; Battista, T. L.; Ragogna, P. J. Lewis Base Sequestered Chalcogen Dihalides: Synthetic Sources of ChX<sub>2</sub> (Ch = Se, Te; X = Cl, Br). *Chem. - Eur. J.* **2009**, *15*, 10263–10271.
- (43) Jenkins, H. A.; Dumaresque, C. L.; Vidovic, D.; Clyburne, J. A. C. The coordination chemistry of o,o'-i-Pr<sub>2</sub>C<sub>6</sub>H<sub>3</sub>-bis(imino)-acenaphthene to group 13 trihalides. *Can. J. Chem.* **2002**, *80*, 1398–1403.
- (44) Schumann, H.; Hummert, M.; Lukoyanov, A. N.; Fedushkin, I. L. Monomeric Alkylaluminum Complexes (dpp-BIAN)AlR<sub>2</sub> (R = Me, Et, <sup>i</sup>Bu) Supported by the Rigid Chelating Radical-Anionic 1,2-Bis[(2,6-diisopropylphenyl)imino]acenaphthene Ligand (dpp-BIAN). *Organometallics* **2005**, *24*, 3891–3896.
- (45) Lukoyanov, A. N.; Fedushkin, I. L.; Hummert, M.; Schumann, H. Aluminum complexes with mono- and dianionic diimine ligands. *Russ. Chem. Bull.* **2006**, *55*, 422–428.
- (46) Schumann, H.; Hummert, M.; Lukoyanov, A. N.; Fedushkin, I. L. Sodium Cation Migration Above the Diimine  $\pi$ -System of Solvent Coordinated dpp-BIAN Sodium Aluminum Complexes (dpp-BIAN = 1,2-Bis[(2,6-diisopropylphenyl)imino]acenaphthene). *Chem. - Eur. J.* **2007**, *13*, 4216–4222.
- (47) Lukoyanov, A. N.; Fedushkin, I. L.; Schumann, H.; Hummert, M. Monoalkylaluminum Complexes Stabilized by a Rigid Dianionic Diimine Ligand: Synthesis, Solid State Structure, and Dynamic Solution Behaviour of (dpp-BIAN)AlR (R = Me, Et, <sup>i</sup>Bu). *Z. Anorg. Allg. Chem.* **2006**, *632*, 1471–1476.
- (48) Baker, R. J.; Jones, C.; Kloth, M.; Mills, D. P. The reactivity of gallium(I) and indium(I) halides towards bipyridines, terpyridines, imino-substituted pyridines and bis(imino)acenaphthenes. *New J. Chem.* **2004**, *28*, 207–213.
- (49) Fedushkin, I. L.; Lukoyanov, A. N.; Ketkov, S. Y.; Hummert, M.; Schumann, H. [(dpp-Bian)Ga-Ga(dpp-Bian)] and [(dpp-Bian)Zn-Ga(dpp-Bian)]: Synthesis, Molecular Structures, and DFT Studies of These Novel Bimetallic Molecular Compounds. *Chem. - Eur. J.* **2007**, *13*, 7050–7056.
- (50) Wang, J.; Ganguly, R.; Yongxin, L.; Diaz, J.; Soo, H. S.; Garcia, F. A multi-step solvent-free mechanochemical route to indium(III) complexes. *Dalton Trans.* **2016**, *45*, 7941–7946.
- (51) Vasudevan, K. V.; Cowley, A. H. New bimetallic complexes supported by a tetrakis(imino)pyracene (TIP) ligand. *New J. Chem.* **2011**, *35*, 2043–2046.
- (52) Shi, Y. X.; Xu, K.; Clegg, J. K.; Ganguly, R.; Hirao, H.; Frišćić, T.; García, F. The First Synthesis of the Sterically Encumbered Adamantoid Phosphazane P<sub>4</sub>(N<sup>t</sup>Bu)<sub>6</sub>: Enabled by Mechanochemistry. *Angew. Chem., Int. Ed.* **2016**, *55*, 12736–12740.
- (53) Shao, H.; Muduli, S. K.; Tran, P. D.; Soo, H. S. Enhancing electrocatalytic hydrogen evolution by nickel salicylaldimine complexes with alkali metal cations in aqueous media. *Chem. Commun.* **2016**, *52*, 2948–2951.
- (54) Gazi, S.; Ng, W. K. H.; Ganguly, R.; Putra Moeljadi, A. M.; Hirao, H.; Soo, H. S. Selective photocatalytic C-C bond cleavage under ambient conditions with earth abundant vanadium complexes. *Chem. Sci.* **2015**, *6*, 7130–7142.
- (55) Muduli, S. K.; Wang, S.; Chen, S.; Ng, C. F.; Huan, C. H. A.; Sum, T. C.; Soo, H. S. Mesoporous cerium oxide nanospheres for the visible-light driven photocatalytic degradation of dyes. *Beilstein J. Nanotechnol.* **2014**, *5*, 517–523.
- (56) Tu, T.; Sun, Z.; Fang, W.; Xu, M.; Zhou, Y. Robust Acenaphthoimidazolydene Palladium Complexes: Highly Efficient Catalysts for Suzuki–Miyaura Couplings with Sterically Hindered Substrates. *Org. Lett.* **2012**, *14*, 4250–4253.
- (57) Gottumukkala, A. L.; Teichert, J. F.; Heijnen, D.; Eisink, N.; van Dijk, S.; Ferrer, C.; van den Hoogenband, A.; Minnaard, A. J. Pd-Diimine: A Highly Selective Catalyst System for the Base-Free Oxidative Heck Reaction. *J. Org. Chem.* **2011**, *76*, 3498–3501.
- (58) Rightmire, N. R.; Hanusa, T. P. Advances in organometallic synthesis with mechanochemical methods. *Dalton Trans.* **2016**, *45*, 2352–2362.

(59) Garay, A. L.; Pichon, A.; James, S. L. Solvent-free synthesis of metal complexes. *Chem. Soc. Rev.* **2007**, *36*, 846–855.

(60) Despite the synthesis of **5b** being reported in our previous study, its structural features when crystallized in *N,N*-dimethylformamide (DMF) are discussed in the present paper.

(61) Whittlesey, B. R.; Ittycheriah, I. P. Trichlorobis-(tetrahydrofuran)indium(III). *Acta Crystallogr., Sect. C: Cryst. Struct. Commun.* **1994**, *50*, 693–695.

(62) Connelly, N. G.; Geiger, W. E. Chemical Redox Agents for Organometallic Chemistry. *Chem. Rev.* **1996**, *96*, 877–910.

(63) Viganò, M.; Ferretti, F.; Caselli, A.; Ragaini, F.; Rossi, M.; Mussini, P.; Macchi, P. Easy Entry into Reduced Ar-BIANH<sub>2</sub> Compounds: A New Class of Quinone/Hydroquinone-Type Redox-Active Couples with an Easily Tunable Potential. *Chem. - Eur. J.* **2014**, *20*, 14451–14464.

(64) Fedushkin, I. L.; Sokolov, V. G.; Piskunov, A. V.; Makarov, V. M.; Baranov, E. V.; Abakumov, G. A. Adaptive behavior of a redox-active gallium carbenoid in complexes with molybdenum. *Chem. Commun.* **2014**, *50*, 10108–10111.

(65) Allan, C. J.; Cooper, B. F. T.; Cowley, H. J.; Rawson, J. M.; Macdonald, C. L. B. Non-Innocent Ligand Effects on Low-Oxidation-State Indium Complexes. *Chem. - Eur. J.* **2013**, *19*, 14470–14483.

(66) Klein, R. A.; Elsevier, C. J.; Hartl, F. Redox Properties of Zerovalent Palladium Complexes Containing  $\alpha$ -Diimine and *p*-Quinone Ligands. *Organometallics* **1997**, *16*, 1284–1291.

(67) Jurca, T.; Lummiss, J.; Burchell, T. J.; Gorelsky, S. I.; Richeson, D. S. Capturing In<sup>+</sup> Monomers in a Neutral Weakly Coordinating Environment. *J. Am. Chem. Soc.* **2009**, *131*, 4608–4609.

(68) Chen, F.; Ma, G.; Cavell, R. G.; Terskikh, V. V.; Wasylishen, R. E. Solid-state <sup>115</sup>In NMR study of indium coordination complexes. *Chem. Commun.* **2008**, 5933–5935.

(69) Hamaed, H.; Johnston, K. E.; Cooper, B. F. T.; Terskikh, V. V.; Ye, E.; Macdonald, C. L. B.; Arnold, D. C.; Schurko, R. W. A <sup>115</sup>In solid-state NMR study of low oxidation-state indium complexes. *Chem. Sci.* **2014**, *5*, 982–995.

(70) Chen, F.; Ma, G.; Bernard, G. M.; Cavell, R. G.; McDonald, R.; Ferguson, M. J.; Wasylishen, R. E. Solid-State <sup>115</sup>In and <sup>31</sup>P NMR Studies of Triarylphosphine Indium Trihalide Adducts. *J. Am. Chem. Soc.* **2010**, *132*, 5479–5493.

(71) Becke, A. D. Density-functional exchange-energy approximation with correct asymptotic behavior. *Phys. Rev. A: At., Mol., Opt. Phys.* **1988**, *38*, 3098–3100.

(72) Lee, C.; Yang, W.; Parr, R. G. Development of the Colle-Salvetti correlation-energy formula into a functional of the electron density. *Phys. Rev. B: Condens. Matter Mater. Phys.* **1988**, *37*, 785–789.

(73) Becke, A. D. Density-functional thermochemistry. III. The role of exact exchange. *J. Chem. Phys.* **1993**, *98*, 5648–5652.

(74) Hehre, W. J.; Radom, L.; Pople, J. A.; Schleyer, P. V. R. *Ab Initio Molecular Orbital Theory*; Wiley: New York, 1986.

(75) Hay, P. J.; Wadt, W. R. Ab initio effective core potentials for molecular calculations. Potentials for the transition metal atoms Sc to Hg. *J. Chem. Phys.* **1985**, *82*, 270–283.

(76) Marenich, A. V.; Cramer, C. J.; Truhlar, D. G. Universal Solvation Model Based on Solute Electron Density and on a Continuum Model of the Solvent Defined by the Bulk Dielectric Constant and Atomic Surface Tensions. *J. Phys. Chem. B* **2009**, *113*, 6378–6396.

(77) Frisch, M. J.; Trucks, G. W.; Schlegel, H. B.; Scuseria, G. E.; Robb, M. A.; Cheeseman, J. R.; Scalmani, G.; Barone, V.; Mennucci, B.; Petersson, G. A.; Nakatsuji, H.; Caricato, M.; Li, X.; Hratchian, H. P.; Izmaylov, A. F.; Bloino, J.; Zheng, G.; Sonnenberg, J. L.; Hada, M.; Ehara, M.; Toyota, K.; Fukuda, R.; Hasegawa, J.; Ishida, M.; Nakajima, T.; Honda, Y.; Kitao, O.; Nakai, H.; Vreven, T.; Montgomery, J. A., Jr.; Peralta, J. E.; Ogliaro, F.; Bearpark, M.; Heyd, J. J.; Brothers, E.; Kudin, K. N.; Staroverov, V. N.; Kobayashi, R.; Normand, J.; Raghavachari, K.; Rendell, A.; Burant, J. C.; Iyengar, S. S.; Tomasi, J.; Cossi, M.; Rega, N.; Millam, J. M.; Klene, M.; Knox, J. E.; Cross, J. B.; Bakken, V.; Adamo, C.; Jaramillo, J.; Gomperts, R.; Stratmann, R. E.; Yazyev, O.; Austin, A. J.; Cammi, R.; Pomelli, C.; Ochterski, J. W.; Martin, R. L.;

Morokuma, K.; Zakrzewski, V. G.; Voth, G. A.; Salvador, P.; Dannenberg, J. J.; Dapprich, S.; Daniels, A. D.; Farkas, O.; Foresman, J. B.; Ortiz, J. V.; Cioslowski, J.; Fox, D. J. *Gaussian 09*, revision D.01; Gaussian, Inc.: Wallingford, CT, 2009.